AD-A036 387 NAVAL SURFACE WEAPONS CENTER DAHLGREN LAB VA F/G 19/1
METHOD FOR A SIMPLE ESTIMATE OF THE MAGNITUDE OF FLECTROMAGNETI--ETC(U)
DEC 76 J H HALBERSTEIN
UNCLASSIFIED NSWC/DL-TR-3587 NL

1 OF 1
AD A036387

END
DATE FILMED
8-77

NSWC/DL TR-3587

# METHOD FOR A SIMPLE ESTIMATE OF THE MAGNITUDE OF ELECTROMAGNETIC FIELDS IN A SHIPBOARD ENVIRONMENT

by
J. H. HALBERSTEIN
Electronics Systems Department



DECEMBER 1976

Approved for public release; distribution unlimited

NAVAL SURFACE WEAPONS CENTER
Dahlgren Laboratory
Dahlgren, Virginia 22448

nswc

NAVAL SURFACE WEAPONS CENTER
DAHLGREN LABORATORY
Dahlgren, Virginia
22448

D. M. Agnew, Jr., Capt., USN
OIC and Assistant Commander

J. H. Mills, Jr.
Associate Technical Director

UNCLASSIFIED

SECURITY CLASSIFICATION OF THIS PAGE (When Data Entered)

| REPORT DOCUMENTATION PAGE | READ INSTRUCTIONS BEFORE COMPLETING FORM |
|---|---|
| 1. REPORT NUMBER<br>TR-3587 (14) NSWC/DL-TR-3587 | 2. GOVT ACCESSION NO. 3. RECIPIENT'S CATALOG NUMBER |
| 4. TITLE (and Subtitle)<br>(6) Method for a Simple Estimate of the Magnitude of Electromagnetic Fields in a Shipboard Environment, | 5. TYPE OF REPORT & PERIOD COVERED<br>6. PERFORMING ORG. REPORT NUMBER |
| 7. AUTHOR(s)<br>(10) Joseph H. Halberstein | 8. CONTRACT OR GRANT NUMBER(s)<br>(12) 22 p. |
| 9. PERFORMING ORGANIZATION NAME AND ADDRESS<br>Naval Surface Weapons Center<br>Dahlgren Laboratory<br>Dahlgren, Virginia 22448 | 10. PROGRAM ELEMENT, PROJECT, TASK AREA & WORK UNIT NUMBERS<br>NELC Task Area No.<br>N0095376WR00034 |
| 11. CONTROLLING OFFICE NAME AND ADDRESS<br>Naval Surface Weapons Center<br>Dahlgren Laboratory<br>Dahlgren, Virginia 22448 | 12. REPORT DATE<br>(11) Dec[redacted]76<br>13. NUMBER OF PAGES<br>26 |
| 14. MONITORING AGENCY NAME & ADDRESS (if different from Controlling Office)<br>(9) Technical rept., | 15. SECURITY CLASS. (of this report)<br>Unclassified<br>15a. DECLASSIFICATION/DOWNGRADING SCHEDULE |
| 16. DISTRIBUTION STATEMENT (of this Report)<br>Approved for public release; distribution unlimited. | |
| 17. DISTRIBUTION STATEMENT (of the abstract entered in Block 20, if different from Report) | |
| 18. SUPPLEMENTARY NOTES | |
| 19. KEY WORDS (Continue on reverse side if necessary and identify by block number) | |
| 20. ABSTRACT (Continue on reverse side if necessary and identify by block number)<br>A methodology is proposed which aims at providing simple, rapid, and cost-effective *estimates* of the magnitude of electromagnetic fields in a shipboard environment. In this technical report the method is illustrated by an example involving scattering of plane wave radiation incident at right angles or obliquely on a circular cylinder.<br>(Continued) | |

DD FORM 1 JAN 73 1473 EDITION OF 1 NOV 65 IS OBSOLETE
S/N 0102-014-6601

UNCLASSIFIED

SECURITY CLASSIFICATION OF THIS PAGE (When Data Entered)

391 598

20. (Continued)

It is recommended that the method be developed more fully and applied as first cull in problems of shipboard siting, HERO-, RADHAZ-, EMC-, and operational problems. The relatively small regions of the field requiring better accuracy are then treated in a second cull by the methods developed or under development by the academic community. This procedure promises considerable improvements in cost effectiveness.

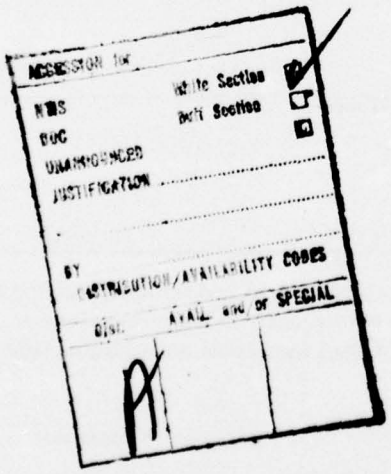

## FOREWORD

The work described in this report was performed in the Systems Compatibility Branch, Systems Effectiveness Division of the Electronic Systems Department under the ITEMA-task funded by the Naval Electronic Laboratory Center under Task Area Number N0095376 WR 00034.

The report was reviewed by Mr. Lloyd Diehl, Dr. John Cavanagh, and Mr. Roger Schirmer.

Released by

L. A. Clayberg, Head
Electronics Systems Department

## TABLE OF CONTENTS

# I. INTRODUCTION

This technical report is intended to describe some of the work done at the Naval Surface Weapons Center, Dahlgren Laboratory in FY-76 on the application of Geometric Theory of Diffraction (GTD) analysis and related methods to shipboard electromagnetic problems.[1] In particular, the work addressed the search for methods which are accurate enough to give useful results, yet simple enough to permit solution of the very complex analysis problems arising in the shipboard electromagnetic environment. As a "testbed" problem, the scattering of electromagnetic radiation from a metallic circular cylinder was chosen. This problem could, for example, represent the scattering of the radiation from a radar antenna by a ship's mast or a whip antenna. The problem to be solved could for instance be as follows: We install a radar antenna in location A on board the ship and a cylindrical mast in location B. We intend to transport hazardous explosives along path c. Will the path c be in an hazardous electromagnetic field? If yes, how can the geometry of A versus B versus c be modified so as to eliminate the hazard? In order to obtain a good appreciation of such problems, it is important to remember that there is a hierarchy of contributions to the total field in any location, which consists of a superposition of (1) direct radiation, (2) radiation reflected from the cylinder and (3) radiation diffracted from the cylinder. In the following sections an attempt will be made to establish the order of magnitude of these contributions.

The estimates described in this report and in the proposed follow-up to this work are designed to be worst-case, i.e., high estimates. The computations are designed to serve as a first, simple, rapid, and cost-effective cull for a large number of field points. In certain regions this estimate will result in high values for the total field. If these values are unacceptable from the HERO, RADHAZ, EMC, or operational point of view, a second cull will be performed for the relatively small number of field points determined by the first cull. The second cull will employ the accurate methods developed or under development by the academic community. This two-step process will optimize the efficiency of the computational procedures.

The effect of the blockage by the cylinder may be divided according to the field regions considered. These may be classified as shadow, half-shadow, and unobstructed regions. In the work reported here we concentrated on the latter two regions, which in most practical problems will make up most of the total field space considered. The ratio between the extent of the total shadow region on the one hand and the half-shadow and unobstructed regions on the other is typically between the orders of magnitude 0.01 and 0.1. Although the problems arising in the shadow region are sometimes very important, we did not address them. In the two-step process described above this region of the electromagnetic field would be handled in the second cull.

The work was accompanied by a literature search, which also permitted us to place our work in perspective with respect to a representative cross section of the published literature. Our testbed problem is simple, compared to the much more complex geometries encountered in a shipboard environment. Yet the literature contains a very large number of papers which in some way treat a subproblem of the above simple problem. The incident field may be a plane, cylindrical, or spherical wave corresponding respectively to a point source at "infinity," a linear source, and a point source "nearby," where the words "infinity" and "nearby" have a meaning only if related to another length, most frequently the wavelength and/or the

diameter of the cylinder. Sometimes complex sources, such as arrays of line sources or special sources such as dipoles are treated. The incident field may be further specialized by its time dependence, CW, pulse, or step function. The problem may be treated as two-dimensional or three-dimensional, as scalar or vectorial. The secondary field treated may be the reflected, diffracted, or refracted field, near field, or far field; the interest may center on blockage of the mainlobe or generation by scatter of new sidelobes, backscatter or bistatic scattering, or special regions of the field such as caustics or transition regions. A further source of differentiation lies in the mathematical methods used for the solution: integral equations method, modal solutions, conformal mapping. Of particular interest are the possible approximations. There, those approximations which permit simple physical analogies, such as geometrical optics, physical optics, geometric theory of diffraction, are particularly appealing because they are helped by intuition based on simple, well-known physical laws. The physical properties of the scattering body (cylinder) range from infinite to zero conductivity (i.e., metal to dielectric) and include complex conductivity (e.g., lossy dielectric). Depending on the relative direction of the polarization of the incident field and the cylinder axis, the boundary conditions may be "soft" or "hard," or an "impedance" boundary condition may apply. Several materials may be involved in the scattering process, such as in scatter from dielectric covered metallic cylinders, or plasma-coated cylinders. Some published papers center not on the scattered field but on an intermediate quantity such as the current induced on the surface of the cylinder. Others concentrate on mathematical properties of functions occurring in the treatment of scattering problems, e.g., cylinder functions, Airy integrals, Fock functions. Finally, sometimes the problem treated in a paper may be more general in one respect and more restrictive in another than our testbed-cylinder scatter problem. For instance, the scattering of a plane wave from a cylinder of arbitrary cross section and axis perpendicular to the incident plane wave would fall into this category.

The above description of the scope of the literature relating, more or less closely, to the testbed problem is by no means exhaustive but may serve as an illustration of the possible number of parameters which may combine in many different ways in the literature.

Considering the large number of parameters, the "sample space" of possible different papers which would apply to the different possible problems occurring in actual situations is enormous. Of course only a small fraction of this sample space has been reported on in the literature.

I would like to end this introduction by mentioning an unbalance I observed in scanning the literature. There is a large number of purely theoretical papers and a far smaller number of experimental papers. This unbalance is at least partly due to the very considerable advances in theory made possible in recent years by the enormous progress in computer science and available computer facilities. However, the need for the interplay between theory and measurement is now as necessary as always.

## II. ESTIMATE OF REFLECTED VERSUS DIFFRACTED POWER

The general GTD solution for scatter from a circular cylinder was published many years ago in a paper by J. B. Keller et al.[2] It involved fairly time-consuming mathematical operations including infinite series.

Our purpose was to obtain an extremely simplified formulation and at the same time an estimate of the price in accuracy of this simplification. We regarded this as an area of things which should be done but which do not show up in detail in the literature. The GTD solution to the cylinder diffraction problem is based on an asymptotic series for the field $U$ of the Luneberg-Kline form

$$U(x, y, z) = e^{ik\psi} \sum_{m=0}^{\infty} \frac{V_m(x, y, z)}{(ik)^m}$$

where $V_m$ is the $m$-th order term of the series, and $k = 2\pi/\lambda$. In the high-frequency limit the series is approximated by the zero-order term for $m = 0$. It depends no longer on $ka$ (where $a$ is the radius of the cylinder) and is recognized as the solution of the EM problem offered by geometrical optics. As $ka$ decreases, the relative values of the higher-order terms, representing diffraction rather than reflection, increase. An examination of the expressions for the $V_m$ coefficients shows that the zero-order term is dominant in our problem for most field points, and for many shipboard environment problems only the first term in the series needs to be considered. This is true for both normal and oblique incidence. For a plane wave impinging normally on a circular cylinder we estimated the ratio $R$ between total diffracted and reflected energy. We use Fock's[3] expression for the width $d$ of the shadow boundary strip

$$d = \sqrt[3]{\frac{\lambda a^2}{\pi}}$$

where $a$ is the radius of curvature of the body in the plane of incidence; i.e., in our case $a$ = radius of the cylinder. Assuming that the diffracted energy is due to the energy falling onto the "region of the shadow boundary" as defined by Fock's equation and assuming further that the optical contribution to the scattered energy is due to the energy falling onto the part of the cylinder surface facing the arriving plane wave, we may arrive at an estimate of the relative importance of the total diffracted EM energy to the total reflected energy:

$$\text{defining } R = \frac{\text{reflected energy}}{\text{diffracted energy}} \approx R_1$$

We obtain (see Appendix A1, Equation A1-3)

$$R_1 = \left(\frac{ak}{2}\right)^{1/3} \tag{1}$$

where $R_1$ is an approximation for the desired ratio. Clearly if $R_1$ is large we shall be able to simplify many problems considerably by neglecting the higher-order diffraction terms in comparison with the reflection term.

Equation (1) is evaluated in Appendix A1 in Table A1-1 for various values of $ka$ ($a$ is the radius of the cylinder) between $ka = 50$ and $ka = 2$. As expected, when the diameter of the cylinder decreases or the wavelength increases, the relative contribution of diffraction in the total scattering process rises as compared with reflection. However, it is obvious that, since the thinner cylinder interacts less than a large-diameter cylinder with the incoming radiation, the total diffracted power decreases with cylinder diameter. This situation is shown quantitatively in Appendix A1, Table A1-2. Note that as long as the GTD is valid ($ka \gtrsim 2$) the total reflected power dominates the total diffracted power.

Although the analysis in Appendix A1 assumes a plane wave with incidence perpendicular to the axis of a circular cylinder, it can be extended to oblique incidence and arbitrary smooth, convex cylinder cross sections following the method of Appendix A1 and substituting for the radius $a$ the radius of curvature of the cylinder surface in the plane of incidence of the respective points in the shadow boundary: the width $w$ of the penumbra region will then be

$$w = \left(\frac{2\rho^2}{k}\right)^{1/3}$$

Since most wavefronts may be represented by a "plane wave spectrum," the solutions obtained will be applicable to a fairly general range of problems involving smooth, convex cylinders in near or far fields.

## III. THE CAUSTIC OF A PLANE WAVE IMPINGING ON A RIGHT CIRCULAR CYLINDER AT RIGHT ANGLE TO THE AXIS

Before we approach the estimation of the relative importance of the direct radiation compared to the radiation reflected from the cylinder, it is appropriate to consider the question whether there is a point(s) where the incoming plane wave is concentrated by the reflection from the cylinder or point(s) from where the radiation seems to emanate when seen from the field points. In the latter case, the caustic is called a "virtual" caustic. In our case, only a virtual caustic exists in the interior of the cylinder.

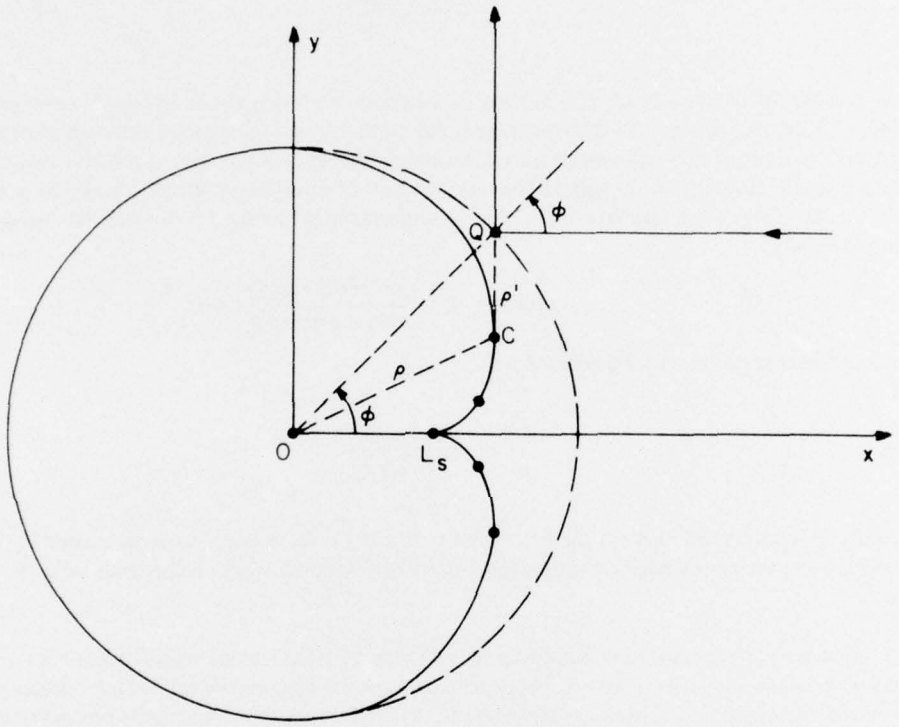


**Figure III-1. Virtual Caustic of a Plane Wave Reflected By a Circular Cylinder**

The virtual caustic of a plane wave parallel to the X-axis obeys the Equations (III-1) below:

$$\left.\begin{aligned} \rho' &= \frac{a\cos\phi}{2} \\ \rho &= a(1 - 0.75\cos^2\phi) \\ \sin(\phi - \alpha) &= \frac{\rho'}{\rho}\sin\phi \end{aligned}\right\} \qquad \text{(III-1)}$$

where $a$ .... radius of the cylinder
$\rho, \alpha$ .... polar coordinates of a point C on the caustic
$\phi, \rho'$ .... see Figure III-1

Equation (III-1) is graphed in Figure III-1 above.

Note that the virtual caustic is not concentrated at a single point or even in a small area of the cylinder but extends throughout its entire width. The intensity of the virtual caustic does however decrease from a maximum on the x-axis to zero on the y-axis. In some cases, e.g., when the field points of interest are far from the cylinder in terms of cylinder diameters, it will be possible to approximate the reflected field by a line source field emanating from $L_S$ (Figure III-1).

It is also worth noting that there will be no constructive or destructive interference between the reflected rays. There will, of course, be interference between the direct and reflected rays.

## IV. ESTIMATE OF DIRECTLY RADIATED VERSUS REFLECTED POWER

A long circular cylinder irradiated by a plane wave at right angles to the cylinder axis will cause reflections from the front face of the cylinder according to the well known equation of geometrical optics (zero-order approximation of GTD):

$$|U_r| \sim \left| A_0 \left(1 + \frac{2r_2}{a \cos\phi}\right)^{-1/2} \right| \qquad \text{(IV-1)}$$

where $a$ .... radius of the cylinder
$r_2$ .... distance to the field point
$\phi$ .... angle of incidence
$|U_r|$ .... reflected field, magnitude
$A_0$ .... amplitude of the incident field

In this case, both constructive and destructive interference will be of importance depending on the field point (F) position. If we call $R_2$ the absolute value of the ratio

$$R_2 = \frac{|\text{direct field}|}{|\text{reflected field}|}$$

we obtain from (IV-1)

$$R_2 \sim \left(1 + \frac{2r_2}{a \cos\phi}\right)^{1/2} \qquad \text{(IV-2)}$$

Note that for $r_2/a >> 1$ it follows that $R_2 >> 1$.

In these field points the reflected energy may be neglected compared to the direct radiation. The value of $|R_2|$ is shown in Table IV-1 below:

Table IV-1. $|R_2| = \dfrac{|\text{Direct Field}|}{|\text{Reflected Field}|}$

| $\phi$ \ $r_2/a$ | 1 | 2 | 5 | 10 | 20 | 50 |
|---|---|---|---|---|---|---|
| 20 | 1.769 | 2.293 | 3.412 | 4.721 | 6.600 | 10.36 |
| 40 | 1.900 | 2.494 | 3.749 | 5.207 | 7.295 | 11.47 |
| 60 | 2.236 | 3.000 | 4.583 | 6.403 | 9.000 | 14.18 |
| 80 | 3.538 | 4.903 | 7.654 | 10.78 | 15.21 | 24.02 |

Note that for large values of $\phi$ and/or $r_2/a$, $R_2$ becomes large and in many cases the reflected field may be neglected compared to the direct field. Since the fields will add vectorially and will in general be at phase angles different from 0 or 180°, the effect of the smaller field will be further diminished. The extension of this analysis to oblique incidence and noncircular, but convex and smooth cylinders is possible with some further work. Also, applying the plane wave spectrum method, nonplanar incident fields may be treated following a similar line of reasoning.

## V. OBLIQUE INCIDENCE, REFLECTED POWER VERSUS DIRECT RADIATION

In the interest of clarity, the proposed approximations have been presented in Sections II and IV for the simplest case of a plane wave at perpendicular incidence on a circular cylinder. We have found that in many circumstances when moderate accuracy is sufficient very simple algebraic expressions will permit us to decide whether the diffraction and reflection due to the cylinder may be neglected, compared to other field contributions, in a given field point. The above cases could be treated with two-dimensional geometry.

In the case of a plane wave at oblique incidence to the cylinder axis, we shall need three-dimensional geometry to describe the problem. Whereas in the problem of Sections II and IV the plane of incidence intersected the cylinder in a circle, at oblique incidence the figure of intersection will be an ellipse. The general case can be reduced to a special (canonical) case if the coordinate system is chosen in a special manner. It is assumed that a contribution of the field at the field point F is obtained by reflection from the cylinder. Calling the point of reflection Q, the x′-axis of the chosen coordinate system will pass through Q while the $z$-axis remains unchanged. For a given direction of incidence and given F the point Q can be determined. An appropriate coordinate transformation will then produce the canonical case. The reflected power as well as the width of the penumbra region can then be determined easily. From them the ratio $R_2$ (Section IV) can be determined. The flowchart for this procedure is given in Appendix A2.

## VI. COMPARISON WITH EXPERIMENT

For verification of the physical optics method used in Sections IV and V, measurements by C.C. H. Tang[4] were used. Figure VI-1 shows the exact solution and measured points for the backscattering widths of infinitely long perfectly conducting circular cylinders with E-fields parallel to the axis (normalized as $\sigma k_0$).

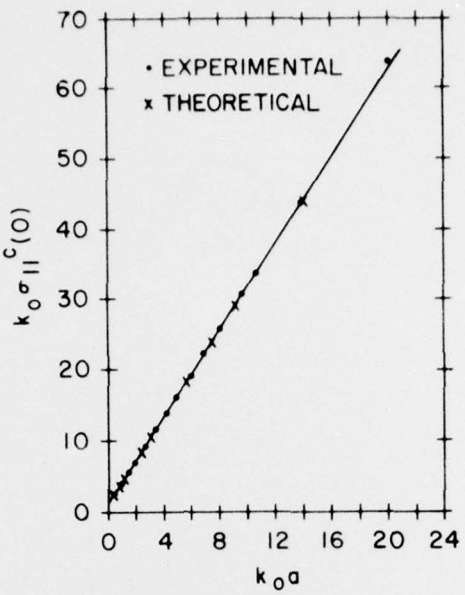


**Figure VI-1. Backscattering from Circular Cylinders after Tang[4]**

The physical optics method may be employed in order to calculate the values of the backscattering widths given in Figure VI-1. The calculation was carried through in Appendix A3. The results of the simple physical optics method agreed in this example with the exact modal solution and the measured values to within 3%.

## VII. REFERENCES


1. Naval Electronics Laboratory Center, Work Request dtd 28 July 1975 to Naval Surface Weapons Center, Dahlgren Laboratory.

2. J. B. Keller, R. M. Lewis and B. Seckler, *Asymptotic Solution of Some Diffraction Problems*, COMM. PURE APPL. MATH., Vol. 9, p. 207-265.

3. V. A. Fock, *Electromagnetic Diffraction and Propagation Problems*, Pergamon Press, 1965, Chapter 1.

4. C. C. H. Tang, *Backscattering From Dielectric – Coated Infinite Cylindrical Obstacles*, J. APPLIED PHYS., Vol. 28, p. 628 (1957).

# APPENDIX A1

# ESTIMATE OF THE TOTAL DIFFRACTED POWER vs. TOTAL INCIDENT POWER

Let a plane wave impinge on a circular cylinder at right angle to the cylinder axis, as shown in Figure A1-1.

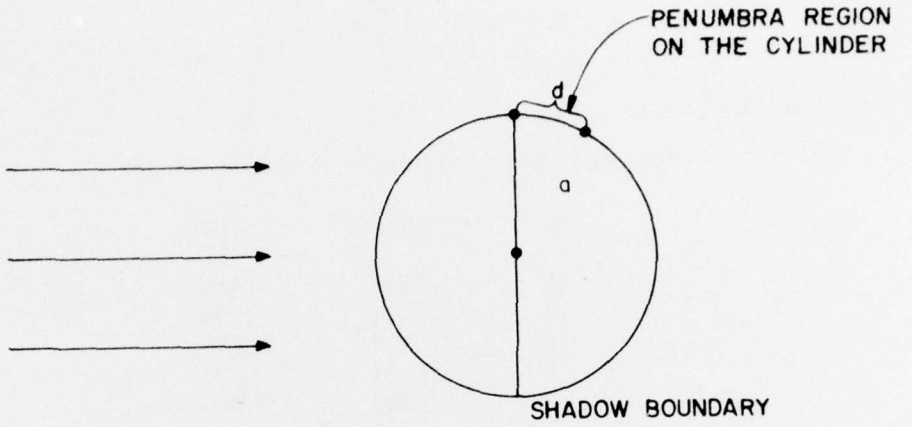


**Figure A1-1. Plane Wave Impinging on a Circular Cylinder**

We want to obtain a coarse estimate of the fraction of the total energy falling on the cylinder which will be diffracted from it. In Figure A1-1 the problem is presented as a two-dimensional cross section of the three-dimensional problem. We assume that $a/\lambda$ is large enough so that the geometrical optics approximation is valid for estimating the reflected power, while the GTD is applicable for the diffracted power. The reflected power ($P_R$) per unit length of the cylinder will be

$$P_R \cong P_0 \cdot 2a \tag{A1-1}$$

where $P_0$ ... power/unit area
$2a$ ... diameter of the cylinder

The total diffracted power ($P_D$) per unit length of the cylinder will be

$$P_D \simeq \int_0^{\xi} P_0 \cdot G^2(\xi)\, d\xi$$

where $G(\xi)$ is a function defined by Fock[4] and $\xi$ is a variable approximately proportional to the distance of the point of diffraction to the shadow boundary. In our coarse estimate it is sufficient to assume that the total diffracted power per unit length is approximately

$$P_D \sim 2P_0 \cdot d \tag{A1-2}$$

where $d$ is the width of the penumbra region on the mantle of the cylinder (Fig. A1-1) $d = (2a^2/k)^{1/3}$ (Reference 4). Let the ratio $P_R/P_D$ be denoted $R$

$$R \approx R_1 = 2aP_0/2P_0\left(\frac{2a^2}{k}\right)^{1/3} = \left(\frac{ak}{2}\right)^{1/3} \tag{A1-3}$$

Thus, we obtain Table (A1-1).

Table A1-1. Ratio of Reflected Power/Diffracted Power

| $ka$ | $R_1 = (ka/2)^{1/3}$ | $R_1$(dB) |
|---|---|---|
| 50 | 2.924 | 4.66 |
| 20 | 2.154 | 3.33 |
| 10 | 1.710 | 2.33 |
| 5 | 1.357 | 1.33 |
| 2 | 1.000 | 0.00 |

As expected, the ratio of reflected power to diffracted power decreases with decreasing diameter/λ. Reflected power equals diffracted power when $ka = 2$. The total power $P$ involved in the scattering process, $P = P_R + P_D$ is obtained by combining Equations (A1-1) and (A1-2).

$$P \sim 2aP_0\left(1 + \left(\frac{2}{ak}\right)^{1/3}\right) \tag{A1-4}$$

Normalized to unit incident power and substituting for $(2/ak)^{1/3}$ from equation (A1-3)

$$\frac{P}{P_0} \sim 2a\left(1 + \frac{1}{R_1}\right) \tag{A1-5}$$

The total scattered power $P$ and the total diffracted power are contrasted in Table A1-2 for constant $k = 1$ and normalized to unit incident power:

Table A1-2. Scattered Power $P$ and Diffracted Power $P_D$

| $ka$ | $P/P_0$ | $P_D/P_0$ | $P_R/P_0$ | $P_D/P_R$ |
|---|---|---|---|---|
| 50 | 134.2 | 34.20 | 100 | 0.342 |
| 20 | 58.56 | 18.56 | 40 | 0.464 |
| 10 | 31.70 | 11.70 | 20 | 0.585 |
| 5 | 17.37 | 7.37 | 10 | 0.737 |
| 2 | 8.- | 4.- | 4 | 1.000 |

Note that, although the relative importance of the diffracted versus reflected power increases as $ka$ decreases, its absolute magnitude decreases for constant $k$ and given incident power density.

# APPENDIX A2

# FLOWCHART FOR THE COMPUTATION OF THE REFLECTED FIELD IN THE CASE OF OBLIQUE INCIDENCE OF A PLANE WAVE ON A CIRCULAR CYLINDER

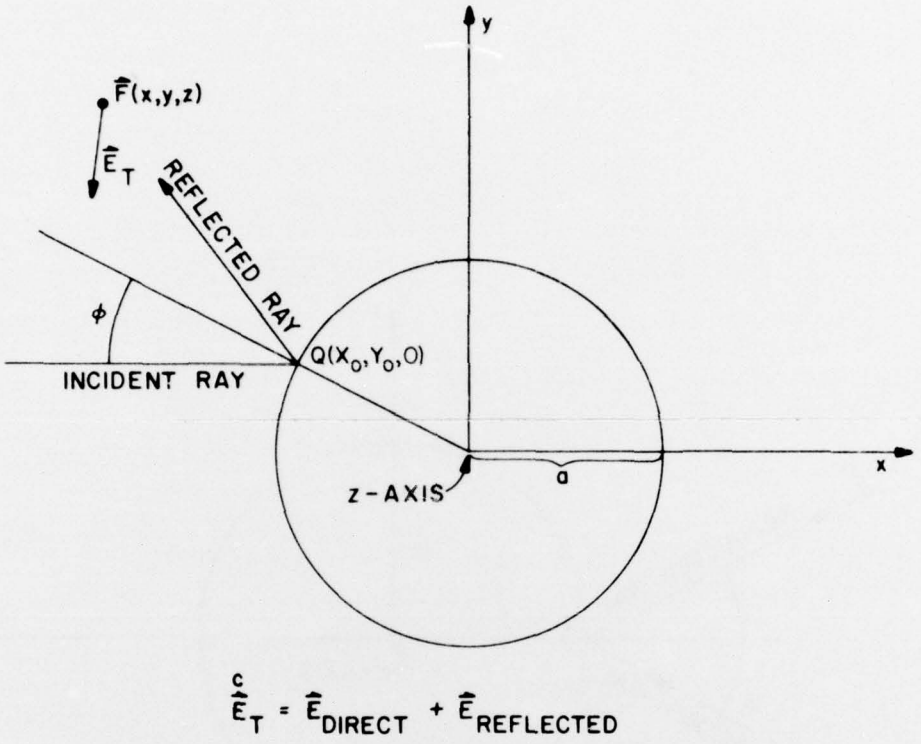


**Figure A2-1. Illustration to Computer Program Flowchart of Figure A2-3.**

The above figure shows the configuration of the incident ray and the ray obliquely reflected from the cylinder. The *z*-axis points out of the plane of the paper. The position of the vector $\bar{F} = \overline{OF}$ is given. Note that for any given vector the coordinate system may be chosen so that $\bar{Q} = \bar{Q}(x_Q, y_Q, 0)$; reflection from a point $\bar{Q}' = \bar{Q}'(x_Q, y_Q, z_Q)$ will be obtained by shifting the coordinate system upward or downward along the *z*-axis to obtain the situation shown in Figure A2-1. Further after $\phi$ is calculated a further coordinate x-formation, a rotation about 0, is performed to bring the point $Q$ onto the x-axis. The canonical position thus produced is shown in Figure A2-2. For all field points where reflected rays pass, the canonical cases may be represented as in Figure A2-2, with only $\phi$ varying. The computation flowchart is shown in Figure A2-3.

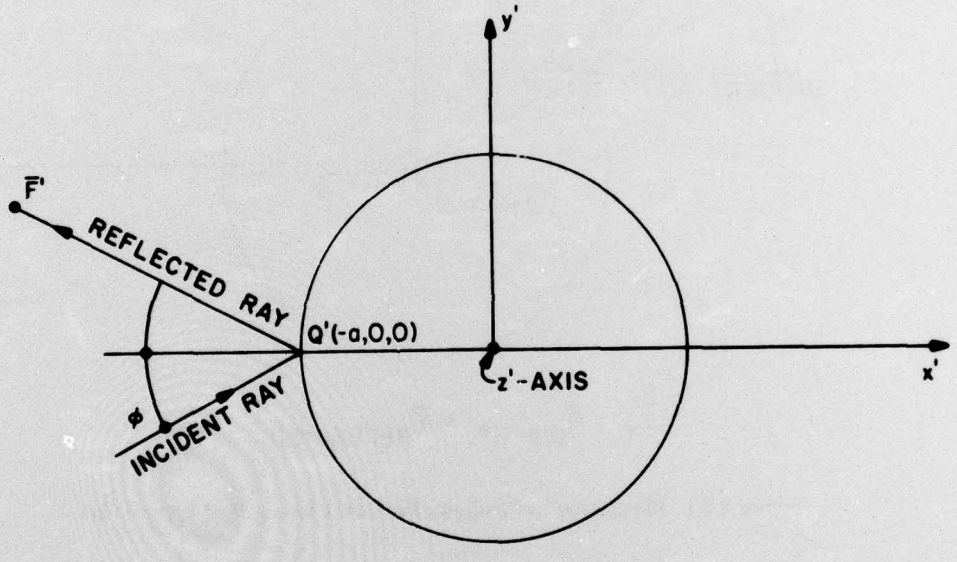


**Figure A2-2. Canonical Case**

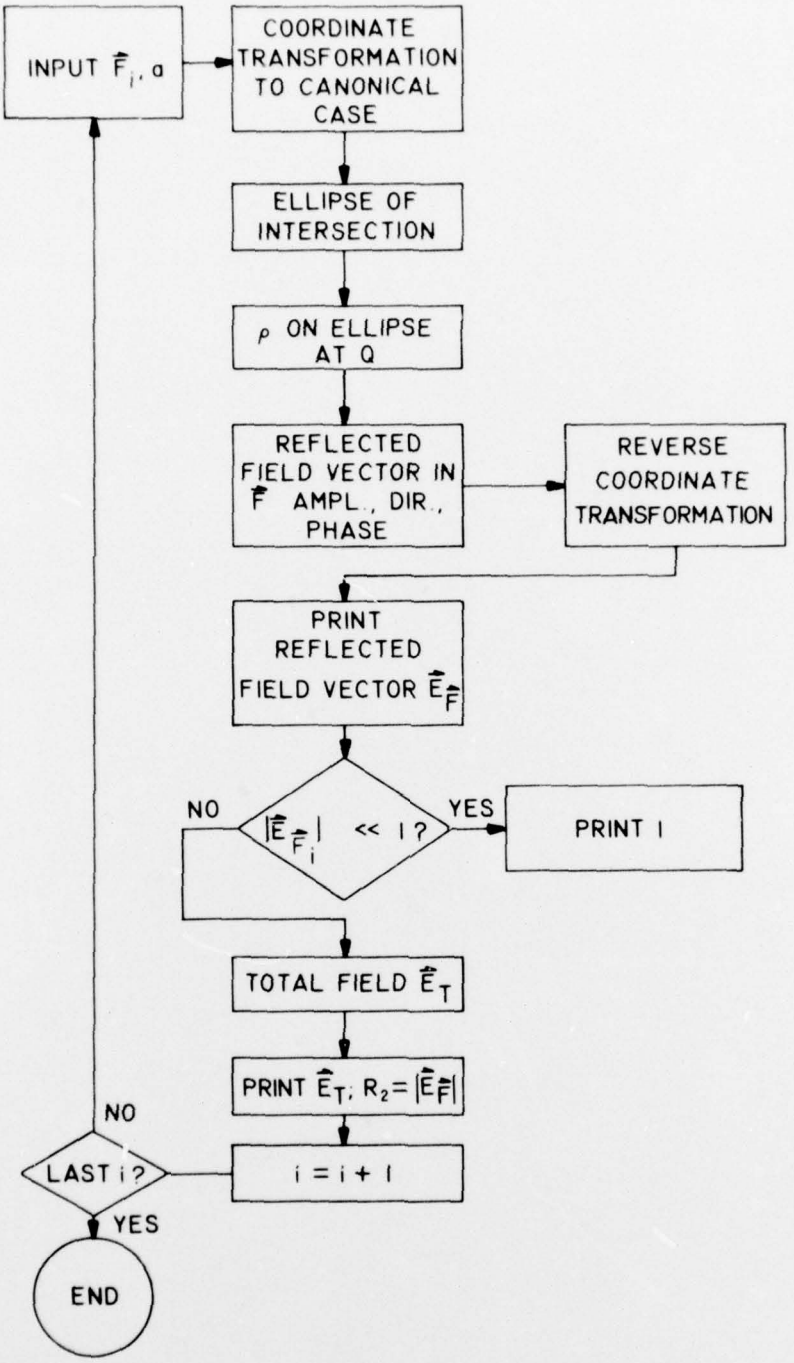


**Figure A2-3. Computation of the Field Reflected From a Cylinder into the Field Point *F* for Oblique Incidence**

# APPENDIX A3

# COMPARISON OF THE PHYSICAL OPTICS RESULTS WITH EXPERIMENT AND EXACT MODAL SOLUTIONS IN BACKSCATTERING FROM A VERY LONG CIRCULAR CYLINDER

For verification of the physical optics method used in Sections IV and V, measurements by C. C. H. Tang[4] were used. In Figure A3-1 the exact solution and measured points for the backscattering widths of an infinitely long perfectly conducting circular cylinder with E-fields parallel to the axis (normalized as $\sigma k_0$) is shown.

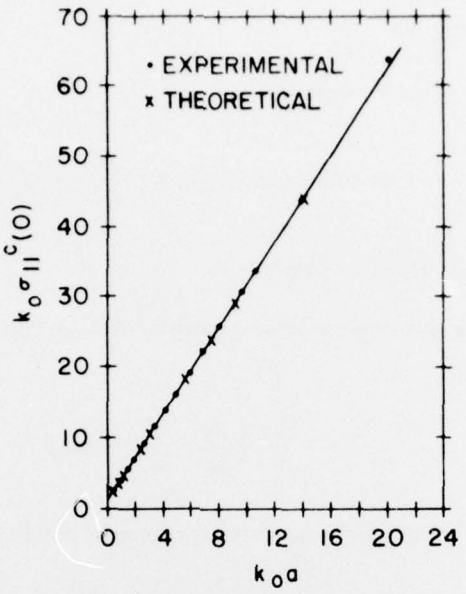


**Figure A3-1. Backscattering from Circular Cylinders after Tang[4]**

The physical optics method may be employed referring to Figure A3-2.

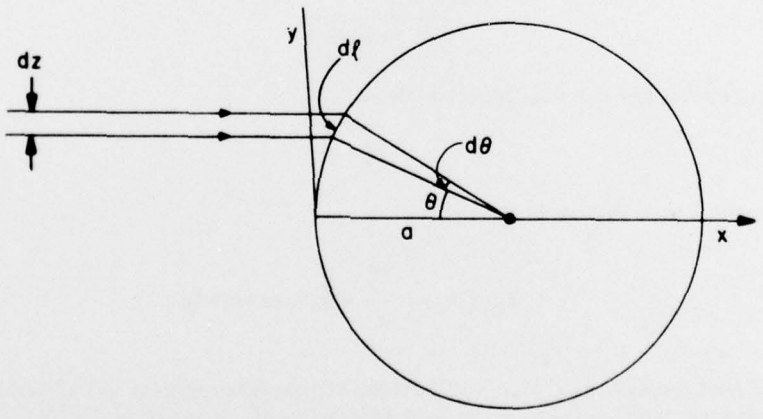


**Figure A3-2. Illustration to the Simplified Analysis of Backscattering from a Circular Cylinder**

$\sigma^c$ is the echoing width; by definition

$$\sigma^c = \frac{2\pi \text{ (scattered power/unit angle)}}{\text{incident power/unit length (along the cylinder diameter)}} \tag{A3-1}$$

$$dl = a d\theta$$

$$\frac{dy}{dl} = \cos\theta$$

$$dy = dl \cos\theta = a \cos\theta d\theta$$

$$\text{incident power/unit length} = \frac{dP}{dy} = \frac{dP}{a \cos\theta d\theta} \tag{A3-2}$$

$dP/dy$ = constant = $c$ ... power/unit length (along $y$)

The power $c$ incident along unit length of $y$ causes power $p'$ scattered from unit length of the cylinder contour:

$$p' = \frac{dp}{dl} = \frac{dp}{dy} \cdot \frac{dy}{dl} = c \cos\theta$$

The power $dp$ incident on the infinitesimal part of the contour $dl$ will be scattered into an angle $2d\theta$:

$$\text{Hence the scattered power/unit angle} = \frac{c \cos\theta \cdot a \cdot d\theta}{2d\theta} \tag{A3-3}$$

and from (A3-1), (A3-2), and (A3-3)

$$\sigma^c = \frac{2\pi c \cos\theta \cdot a}{2c}$$

$$\boxed{\sigma^c = a\pi \cos\theta} \tag{A3-4}$$

For backscatter $\theta = 0$, and Equation (A3-4) becomes

$$\sigma_b^c \simeq a\pi \tag{A3-5}$$

To compare with Figure VI-1 we form

$$k_0\sigma_b^c/k_0 a = \frac{\sigma_b^c}{a} = \pi \text{ (from (A3-5))}$$

From Figure A3-1 we read: $k_0\sigma_b^c/k_0 a \simeq 3.07$ for the experimental values as well as the exact theoretical values. Note that in this case the value obtained with our simple physical optics model gives the precise theoretical and measured values to within 3%.

## DISTRIBUTION

Chief of Naval Material
Department of the Navy
Washington, DC 20360
ATTN: (0343) M. Nunn

Commander
Naval Ship Engineering Center
Washington, DC 20362
ATTN: (6174B) F. Prout
(6174F) P. Law

Commander
Naval Electronic Laboratory Center
San Diego, CA 92152
ATTN: R. Jensen (3)

Commander
Naval Electronic Systems Command
Washington, DC 20360
ATTN: (304) J. Cauffman (3)
(5103) R. Pride
(5102) C. W. Neill
(095) M. Roney
(0953) LCDR R. Witter

Commander
Naval Sea Systems Command
Department of the Navy
Washington, DC 20362
ATTN: (06T) J. McEachen
(3041) H. J. DeMattia

Commander
Naval Air Systems Command
Department of the Navy
Washington, DC 20361
ATTN: (360) F. Lueking

Deputy Director
Electromagnetic Compatibility Analysis Center
North Sedern
Annapolis, MD 21402
ATTN: J. Hodges

Commander
Naval Weapons Center
China Lake, CA 93555
ATTN: (5532) R. Christiansen

Superintendent
Naval Postgraduate School
Monterey, CA 93940
ATTN: Dr. R. W. Adler

Defense Documentation Center
Cameron Station
Alexandria, VA 22314 (12)

Library of Congress
Washington, DC 20540
ATTN: Gift and Exchange Division (4)

Defense Printing Service
Washington Navy Yard
Washington, DC 20374

Local:

| | |
|---|---|
| DF-40 | (2) |
| DF-42 | (40) |
| DX-21 | (2) |
| DX-222 | (6) |
| DX-40 | |